

## Visible Light-Induced Borylation of C-O, C-N, and C-X Bonds

Shengfei Jin, Hang T. Dang, Graham C. Haug, Ru He, Viet D Nguyen,  
Vu T. Nguyen, Hadi D. Arman, Kirk S. Schanze, and Oleg V. Larionov

*J. Am. Chem. Soc.*, **Just Accepted Manuscript** • DOI: 10.1021/jacs.9b12519 • Publication Date (Web): 03 Jan 2020

Downloaded from [pubs.acs.org](https://pubs.acs.org) on January 3, 2020

### Just Accepted

“Just Accepted” manuscripts have been peer-reviewed and accepted for publication. They are posted online prior to technical editing, formatting for publication and author proofing. The American Chemical Society provides “Just Accepted” as a service to the research community to expedite the dissemination of scientific material as soon as possible after acceptance. “Just Accepted” manuscripts appear in full in PDF format accompanied by an HTML abstract. “Just Accepted” manuscripts have been fully peer reviewed, but should not be considered the official version of record. They are citable by the Digital Object Identifier (DOI®). “Just Accepted” is an optional service offered to authors. Therefore, the “Just Accepted” Web site may not include all articles that will be published in the journal. After a manuscript is technically edited and formatted, it will be removed from the “Just Accepted” Web site and published as an ASAP article. Note that technical editing may introduce minor changes to the manuscript text and/or graphics which could affect content, and all legal disclaimers and ethical guidelines that apply to the journal pertain. ACS cannot be held responsible for errors or consequences arising from the use of information contained in these “Just Accepted” manuscripts.

# Visible Light-Induced Borylation of C–O, C–N, and C–X Bonds

Shengfei Jin,<sup>a</sup> Hang. T. Dang,<sup>a</sup> Graham C. Haug,<sup>a</sup> Ru He,<sup>a,b</sup> Viet D. Nguyen,<sup>a</sup> Vu T. Nguyen,<sup>a</sup> Hadi D. Arman,<sup>a</sup> Kirk S. Schanze,<sup>a</sup> and Oleg V. Larionov<sup>\*a</sup>

<sup>a</sup> Department of Chemistry, University of Texas at San Antonio, San Antonio, Texas 78249, United States

<sup>b</sup> Department of Chemistry, University of Florida, Gainesville, Florida 32611, United States

## Supporting Information Placeholder

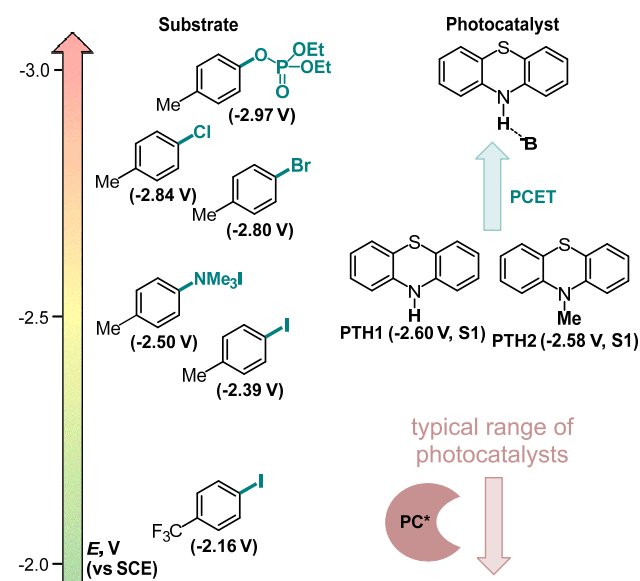
**ABSTRACT:** Boronic acids are centrally important functional motifs and synthetic precursors. Visible light-induced borylation may provide access to structurally diverse boronates, but a broadly-efficient photocatalytic borylation method that can effect borylation of a wide range of substrates, including strong C–O bonds, remains elusive. Herein, we report a general, metal-free visible light-induced photocatalytic borylation platform that enables borylation of electron rich derivatives of phenols and anilines, chloroarenes, as well as other haloarenes. The reaction exhibits excellent functional group tolerance, as demonstrated by the borylation of a range of structurally complex substrates. Remarkably, the reaction is catalyzed by phenothiazine, - a simple organic photocatalyst with MW<200 that mediates the previously unachievable visible light-induced single electron reduction of phenol derivatives with reduction potentials as negative as  $\sim -3$  V vs SCE by a proton-coupled electron transfer mechanism. Mechanistic studies point to the crucial role of the photocatalyst-base interaction.

## Introduction

The importance of boronic acids continues to grow, as new applications emerge in the areas of organic synthesis,<sup>1</sup> catalysis,<sup>2</sup> materials science,<sup>3</sup> drug discovery,<sup>4</sup> and analytical chemistry.<sup>5</sup> Although significant advances have recently been made in synthetic approaches to boronic acids based on transition metal catalysis,<sup>6</sup> main group chemistry<sup>7</sup> and photochemistry,<sup>8-13</sup> various challenges persist and efforts to expand the scope, structural diversity, functional group tolerance, and catalyst availability of emerging organoboron methodologies remain at the forefront of several areas of chemistry. Given the importance of aromatic boronic acids, it is desirable to have a single catalytic platform that enables borylation of all common carbon-heteroatom bonds, including C–O, C–N, and C–X (Cl, Br, I) bonds.

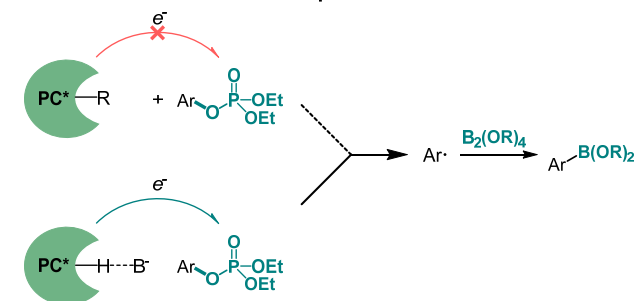
Since the initial reports on the UV light-induced Ar–X and Ar–N borylation,<sup>8</sup> a number of methods were developed that allow for borylation of some of the aryl-heteroatom bonds, in particular, by the groups of Li,<sup>9</sup> Jiao,<sup>10</sup> Schelter,<sup>11</sup> and Studer.<sup>12</sup> Despite the impressive progress, further work is needed to develop a broad photocatalytic platform that encompasses a wide array of diverse C–O, C–N, and C–X bonds and is powered by visible light as a more sustainable and functional group-tolerant source of energy. A desirable photocatalytic platform that can address these limitations would be based on a single, readily available organic photocatalyst that enables borylations of phenols, anilines, as well as chloro-, bromo- and

iodoarenes under visible light. Development of such a broad, visible light-mediated, photocatalytic platform is a major challenge, because of the wide spectrum of reactivities of the aromatic precursors.



- **Challenges:** broad scope (C–O, C–N, C–Cl, C–Br, C–I) without detriment to structural diversity and functional group tolerance, simple organophotocatalytic system operating under visible light

## PCET-enabled visible light-induced borylation of aryl phosphate esters and other low reduction potential substrates



- Visible light-induced borylation of substrates with  $E_{\text{red}} \sim -3.0$  V vs SCE with a simple and inexpensive metal-free photocatalyst with MW < 200
- General visible light-induced photocatalytic platform enables borylation of Ar–O, Ar–Cl, Ar–Br, Ar–I and Ar–N bonds

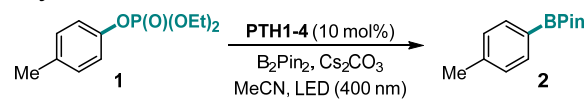
**Figure 1.** Visible light-induced phenothiazine-catalyzed borylation of substrates with low reduction potentials.

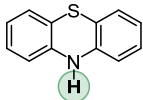
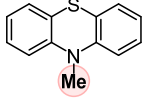
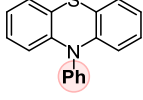
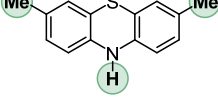
For example, phenols with their strong C–O bond (BDE(C–O) = 110.8 kcal/mol),<sup>14</sup> present a particularly challenging problem for visible light-induced C–O-functionalization. Conversion of phenols to sulfonates (e.g., triflates) is commonly used in transition metal catalysis to facilitate the C–O bond cleavage, but this activation method may be of limited value in photoinduced reactions, because sulfonates tend to undergo the competing S–O bond scission upon photoexcitation or photoinduced single electron transfer, regenerating phenols.<sup>15</sup> In addition, they have low reduction potentials, placing them outside the range of typical photoredox catalysts and requiring exceptionally strongly reducing photocatalysts with suitable photophysical properties that remain to be developed. As a result, a visible light-mediated C–O-borylation has remained elusive, despite its high potential synthetic value. Given these challenges, a conceptually distinct approach to activation and cleavage of the Ar–O bond is required to achieve the C–O-borylation under visible light, even before any progress is made towards a general photocatalytic borylation platform. On the other hand, in the haloarene series, iodoarenes have relatively weak C–I bonds and less negative reduction potentials (e.g.,  $E_{\text{red}} = -2.39$  V vs SCE for *p*-iodotoluene),<sup>16</sup> while chloroarenes, like derivatives of phenols, are much more difficult to reduce (e.g.,  $E_{\text{red}} = -2.84$  V for *p*-chlorotoluene). Hence, the development of a single photocatalytic system that can avoid excessively fast production of aryl radicals from aryl iodides, while also being capable of efficient borylation of chlorides is a significant hurdle.

Addressing the C–O borylation problem first, we turned our attention to aryl phosphate esters as a platform for visible light-mediated activation of the C–O bond in phenols, hypothesizing that they are less likely to undergo a SET-induced P–O bond scission, due to the stronger P–O bond. However, aryl phosphate esters have very negative reduction potentials ( $E_{\text{red}} = -2.97$  V vs SCE for *p*-tolyl diethyl phosphate), necessitating a design of a new photocatalytic system with an enhanced reduction scope. We, therefore, hypothesized that a reductive ability of an appropriately selected organic photocatalyst can be enhanced by a proton-coupled electron transfer (PCET), enabling a photoinduced single electron transfer to substrates with very negative reduction potentials, including electron-rich aryl phosphate esters and chloroarenes (Figure 1). Recent work by Knowles and other groups on proton-coupled electron transfer in photocatalysis has led to the development of new synthetic methods for functionalization of strong bonds.<sup>17</sup> In search of a suitable photocatalyst, we turned our attention to phenothiazine **PTH1** – a common and inexpensive commodity chemical. Although phenothiazine has not been used as a photocatalyst, *N*-alkyl and aryl substituted phenothiazines (e.g., **PTH2** and **PTH3**, Table 1) have recently attracted attention as efficient metal-free photocatalysts in polymer chemistry and organic synthesis.<sup>18</sup> *N*-Substituted phenothiazines **PTH2** and **PTH3** have relatively strongly reducing singlet excited states (Table 1) that allow for production of alkyl and aryl radicals from more easily reducible C–X bonds (e.g. electron deficient haloarenes and  $\alpha$ -haloesters). Although phenothiazine **PTH1** and the *N*-substituted analogues **PTH2** and **PTH3** have very close excited state reduction potentials (Table 1), we hypothesized that phenothiazine **PTH1** can engage in a photoinduced PCET process with aryl phosphates in the presence of an appropriate base, effectively enhancing its reduction strength via this distinctly different photoactivation mechanism, and enabling the downstream borylation via a homolytic substitution with a diboron reagent. Given the potentially broad utility of a visible light-driven metal-free photocatalytic system with an adjustable

reduction potential, **PTH1** photocatalysis can inspire the development of other catalytic systems based on this concept.

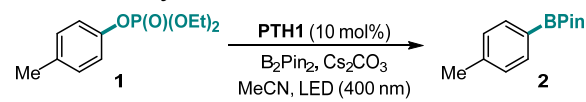
**Table 1. Influence of the Substituents in PTH1-4 on the Catalyst Performance.**<sup>a</sup>



Catalyst	$E_{\text{ox}}(\text{PTH}^+/\text{PTH}^{\bullet}), \text{V}$ (SCE)	Yield, %
 <b>PTH1</b>	-2.60	<b>64</b>
 <b>PTH2</b>	-2.58	12
 <b>PTH3</b>	-2.51	10
 <b>PTH4</b>	-2.71	<b>68</b>

<sup>a</sup> Reaction conditions: phosphate **1** (0.2 mmol), **PTH1-4** (10 mol%),  $\text{B}_2\text{Pin}_2$  (0.6 mmol),  $\text{Cs}_2\text{CO}_3$  (0.6 mmol), MeCN (2 mL), LED light (400 nm), 20 h. Yields were determined by <sup>1</sup>H NMR spectroscopy with 1,4-dimethoxybenzene as an internal standard.

**Table 2. Reaction Conditions for the Visible Light-Driven C–O Borylation.**<sup>a</sup>



Entry	Variations from standard conditions	Yield, %
1	none	64 (78 <sup>b</sup> , 83 <sup>c</sup> )
2	no light	0
3	no <b>PTH1</b>	0
4	no $\text{Cs}_2\text{CO}_3$	0
5	with water (1 equiv.), 10 h	63
6	with 18-crown-6 (1 equiv.), 10 h	60
7	$\text{K}_3\text{PO}_4$ instead of $\text{Cs}_2\text{CO}_3$	30
8	2 equiv. $\text{B}_2\text{pin}_2$	52
9	Tolyl triflate instead of <b>1</b>	37 <sup>d</sup>

<sup>a</sup> Reaction conditions: see footnote for Table 1. <sup>b</sup> Isolated yield for a reaction in the presence of water (1 equiv.). <sup>c</sup> Isolated yield after 36 h. <sup>d</sup> *p*-Cresol was also formed in 54% yield.

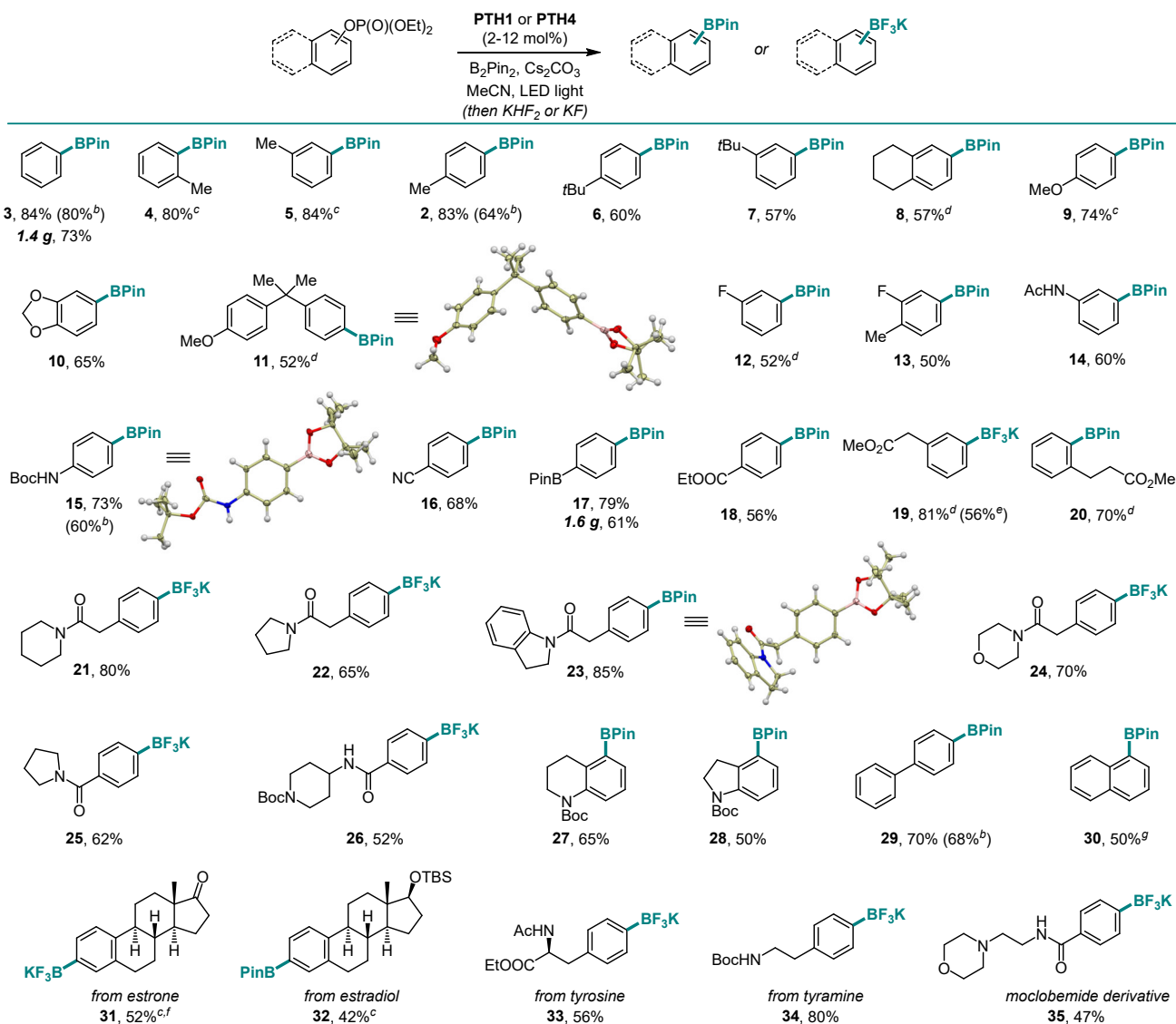
## Results and Discussion

Our studies revealed that the unsubstituted catalyst **PTH1** was uniquely active as a photocatalyst for the borylation of aryl phosphate **1**, with Cs<sub>2</sub>CO<sub>3</sub> as a base (Table 1), while a mere substitution of the *N*-hydrogen atom with a methyl or phenyl group (**PTH2** and **PTH3**) led to a substantial decrease in the catalytic activity. This result is striking, given the comparable excited state redox properties of the *N*-substituted phenothiazines (Table 1). The structurally similar *NH*-phenothiazine **PTH4** showed a slightly improved performance, likely due to the stronger reducing character of the more electron rich core. Notably, none of the photocatalysts **PTH1-4** has a sufficiently strongly reducing singlet excited state to effect the reduction of the electron-rich phosphate **1** ( $E_{\text{red}} = -2.97$  V). The borylation product **2** was not formed in the absence of light, **PTH1**, or cesium carbonate (Table 2). Hypothesizing that addition of reagents that improved solu-

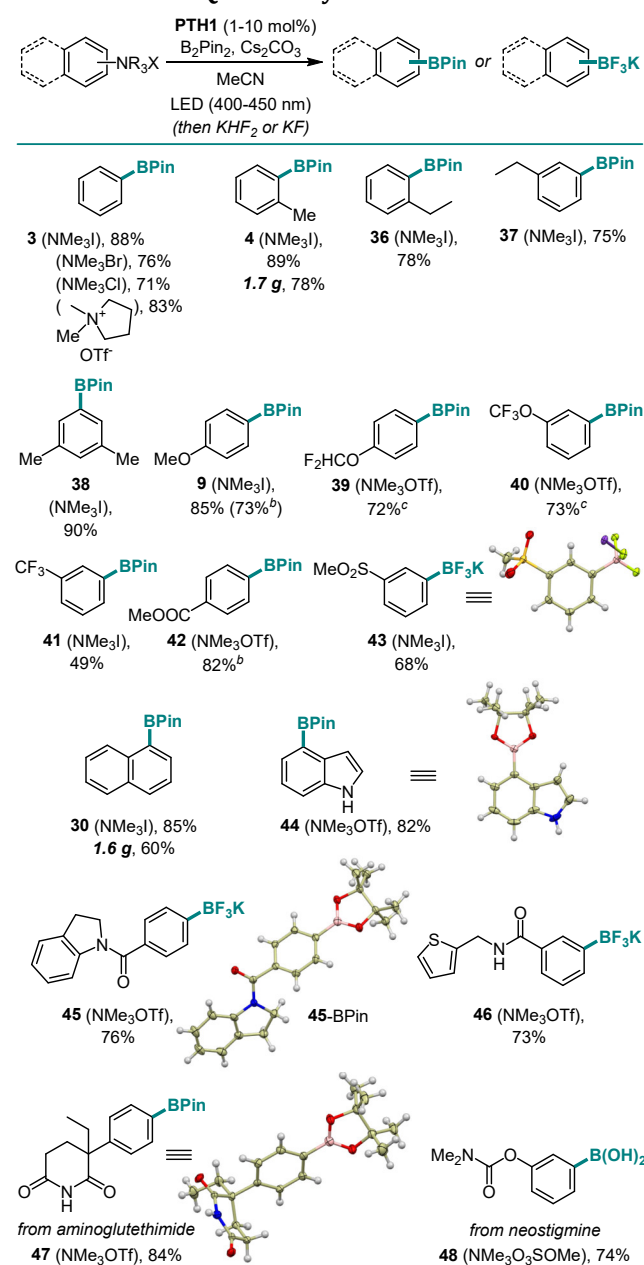
bility and phase transfer of the base would accelerate the borylation, we tested water and 18-crown-6 and observed a faster reaction (Table 2, entries 5 and 6, also see SI) and a higher yield (Table 3, product **2**), pointing to the important role of the base in the catalytic process. Other bases were also able to mediate the borylation (entry 7), with cesium carbonate showing an optimal performance. The borylation can be carried out a lower loading of B<sub>2</sub>Pin<sub>2</sub>, albeit with a reduced conversion (entry 8). As anticipated, replacing phosphate **1** with the corresponding triflate led to a substantially reduced yield and a predominant S–O bond scission (entry 9).

We further proceeded with the evaluation of the scope of the photocatalytic C–O borylation of phosphate esters (Table 3). Electron-rich phosphates, e.g., **2-11** were readily borylated, including those bearing strongly donating alkoxy groups. Medicinally relevant fluoro group (**12** and **13**), as well as amide (**14**) and carbamate (**15**) were also tolerated.

**Table 3. Scope of the Visible Light-Induced C–O Borylation Reaction.<sup>a</sup>**



<sup>a</sup> Reaction conditions: phosphate ester (0.2 mmol), B<sub>2</sub>Pin<sub>2</sub> (0.6 mmol), Cs<sub>2</sub>CO<sub>3</sub> (0.6 mmol), **PTH1** or **PTH4** (2–12 mol%), MeCN (2 mL), LED light (400 or 420 nm). <sup>b</sup> B<sub>2</sub>Pin<sub>2</sub> (0.4 mmol). <sup>c</sup> In the presence of water (1 equiv.). <sup>d</sup> **PTH4** was used. <sup>e</sup> B<sub>2</sub>Pin<sub>2</sub> (0.3 mmol). <sup>f</sup> The keto group in the phosphate ester was protected as an acetal that was removed concomitantly with conversion to trifluoroborate **31**. <sup>g</sup> 450 nm.

**Table 4. Scope of the Visible Light-Induced C–N Borylation Reaction of Quaternary Ammonium Salts.<sup>a</sup>**

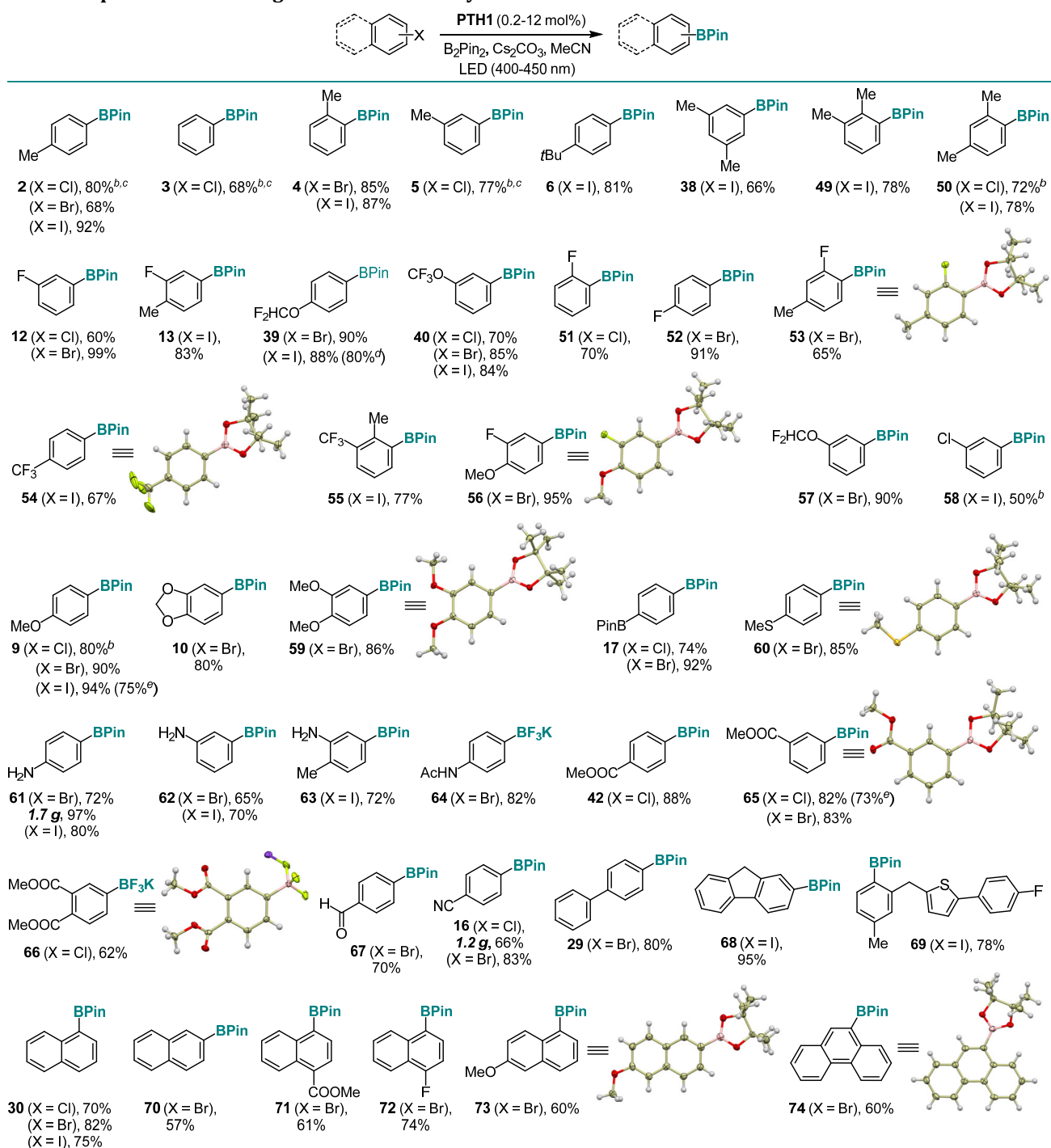
<sup>a</sup> Reaction conditions: see footnote for Table 3. <sup>b</sup>  $B_2Pin_2$  (0.3 mmol). <sup>c</sup> The salt was prepared in situ by stirring with  $MeOTf$  (3.2 equiv.) for 20 min at rt before adding  $B_2Pin_2$  and **PTH1**.

Phosphates with electron-withdrawing groups (e.g., cyano, boryl, ester groups, **16–18**) were equally suitable substrates. All substitution patterns (*o*-, *m*-, *p*-) were tolerated (**18–20**), and gram-scale syntheses were readily performed (**3** and **17**). Similarly, phosphates bearing various N-heterocyclic substituents were converted to the corresponding boronic esters **21–28** in good yields. Furthermore, biphenyl and naphthalene-derived phosphates were readily borylated (**29–30**), suggesting that the reaction can be applicable to polyaromatic systems. Derivatives of estrone, estradiol, tyrosine, tyramine and moclobemide were subjected to the photoinduced C–O borylation and afforded boronates **31–35**, indicating that the new method can be used for borylation of naturally-occurring and medically-relevant phenols. Catalysts **PTH1** and **PTH4** both performed well, and longer wavelength LED light (420 and 450 nm) was also used with success. The optimal catalyst

loading was in the 10–12 mol% range, but a lower (2 mol%) loading is possible for more reactive substrates (e.g., **16**). Furthermore, the borylation products can be isolated as organotrifluoroborate salts<sup>19</sup> as a part of the work-up procedure, further enhancing the practicality of the method.

With the C–O borylation optimized, we were curious to test the performance of the new photocatalytic method on other strong carbon–heteroatom bonds. In particular, functionalization of the strong Ar–N bonds has remained a challenge. Our previous work showed that the C–N-borylation of quaternary arylammonium salts is feasible under UV light irradiation.<sup>8</sup> However, a visible light-mediated C–N-borylation of quaternary arylammonium salts has remained elusive. Initial experiments with phenyltrimethylammonium halides (chlorides, bromides and iodides) demonstrated that the **PTH1**-photocatalyzed C–N-borylation proceeds smoothly (**3**, Table 4). Furthermore, in contrast to the UV light-induced reaction that required iodide and bromide as counteranions, the visible light-mediated reaction is insensitive to the counteranion, and proceeds equally well with all halide salts, as well as triflates and methylsulfates. Other *N*-alkyl groups were also tolerated in the ammonium residue. We further investigated the scope of the reaction with a variety of quaternary arylammonium salts. Substituents in the *ortho*, *meta*, and *para* positions were well-tolerated (**4**, **9**, **37–41**). Substrates bearing medically-relevant fluorine-containing groups ( $CF_3$ ,  $CF_3O$ ,  $F_2HCO$ ) were readily borylated (**39–41**), in addition to ester and sulfone groups (**42**, **43**), as well as a naphthalene salt (**30**). Heterocycle-containing products **44–46** were obtained in good yields. Furthermore, the C–N-borylation performed well in the molecular setting of active pharmaceutical ingredients (API), allowing for preparation of borylated derivatives of aminoglutethimide (Cytadren, **47**) and neostigmine (Prostigmin, **48**). The prerequisite quaternary arylammonium salts can be prepared in situ by brief pretreatment of the corresponding aniline or *N*-alkylaniline with  $MeOTf$ . The reaction can be readily performed on gram scale (e.g., boronates **4** and **30**). As with the C–O-borylation, the products can be isolated as organotrifluoroborate salts or boronic acids. Quaternary arylammonium salts were generally more reactive than phosphate esters, and 1–5 mol% **PTH1** was sufficient to effect the borylation for most of the substrates. On the mechanistic level, the insensitivity of the visible light-mediated borylation of the quaternary ammonium salts to the counteranion indicated that the reaction does not proceed by the charge transfer from the anion, as it was observed in the UV light-induced reaction.<sup>8</sup>

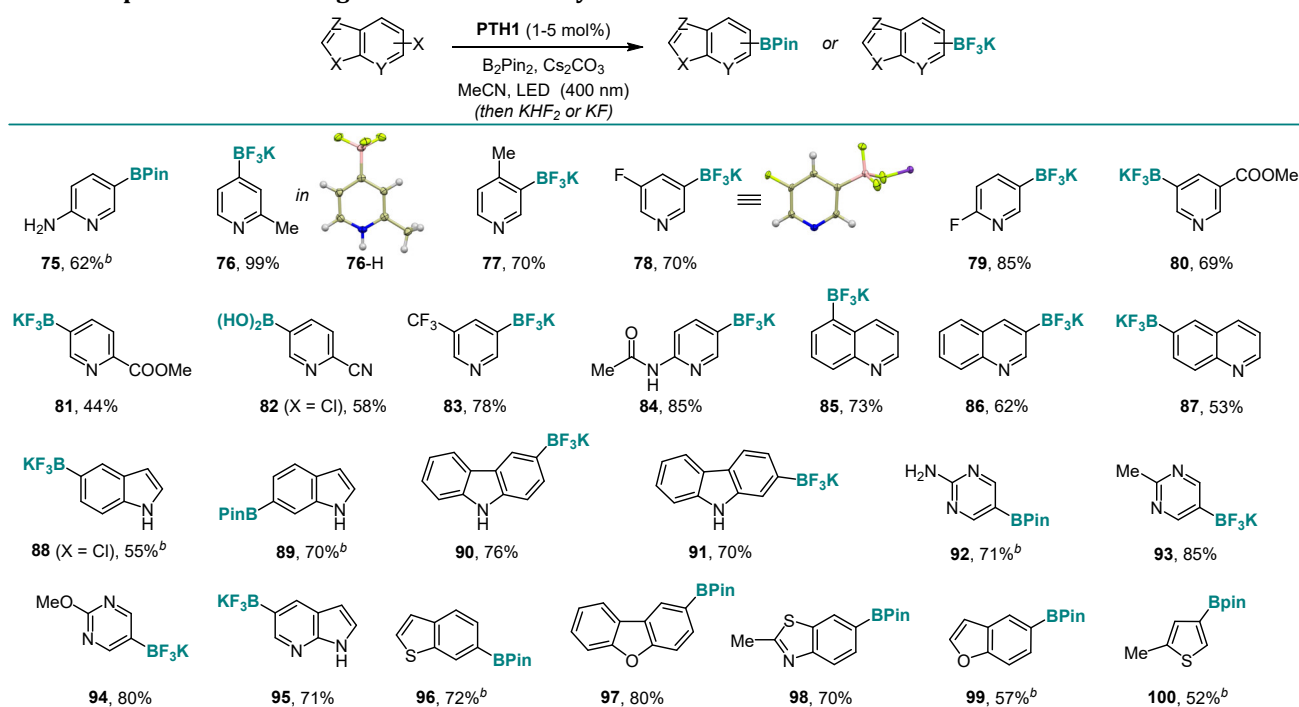
Haloarenes are the most commonly used and readily accessible precursors to boronic acids, and it is important to have a broadly synthetically useful borylation method that can effect the borylation of the three most abundant classes of haloarenes, – chloro-, bromo-, and iodoarenes, in addition to phenols and anilines. We, therefore, tested the performance of the new visible light-mediated **PTH1**-photocatalyzed borylation reaction with chlorobenzene, as well as *para*-chloro-bromo- and iodotoluene (Table 5). Remarkably, an efficient borylation was observed with as little as 0.2–2 mol% **PTH1** for all three classes of halides. Chlorobenzene and *para*-chlorotoluene were converted to the corresponding boronic esters **3** and **2** in good yields, despite their very negative reduction potentials (–2.83 and –2.84 V, respectively). Other alkyl-substituted aryl chlorides, bromides, and iodides were also borylated efficiently (**4–6**, **38**, **49**, **50**), including the electron-rich *ortho,para*-substituted 4-chloro-*m*-xylene ( $E_{red} = -2.92$  V, boronate **50**). The reaction allows for production of fluorinated boronic esters (**12**, **13**, **39**, **40**, **51–57**), as well as

Table 5. Scope of the Visible Light-Induced C-X Borylation Reaction.<sup>a</sup>

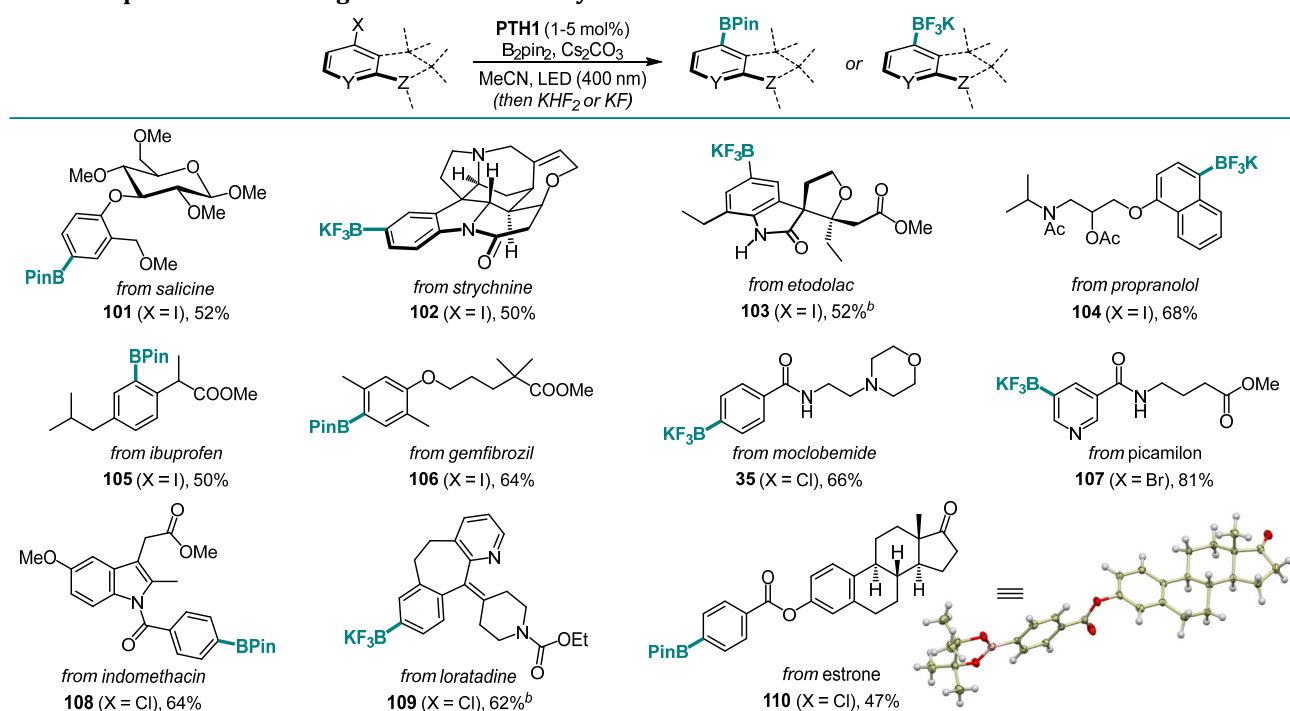
<sup>a</sup> Reaction conditions: see footnote for Table 3 with 2 equiv. B<sub>2</sub>Pin<sub>2</sub>. <sup>b</sup> In the presence of water (1 equiv.). <sup>c</sup> 3 equiv. B<sub>2</sub>Pin<sub>2</sub>. <sup>d</sup> 1.2 equiv. B<sub>2</sub>Pin<sub>2</sub>. <sup>e</sup> 1.5 equiv. B<sub>2</sub>Pin<sub>2</sub>.

for selective borylation of a more readily reduced C-X bond (**58**). Electron-rich 4-chloroanisole was readily reacted, as well as other alkoxy group-containing haloarenes (**9**, **10**, **59**). Boryl, thio, unprotected amino, amido, ester, and other electron-withdrawing groups (**16**, **17**, **60-67**) were well-tolerated. A variety of biaryl and polycyclic haloarenes (**29**, **30**, **68-74**) were converted to the corresponding boronic esters in good yields, independently of the halogen leaving group. Some reactive haloarenes required as little as 0.2 mol% of **PTH1**, and most of the reactions were performed with 1.2-2 equiv. B<sub>2</sub>Pin<sub>2</sub>. The reaction can be readily carried out on a gram scale (**16**, **61**).

Heterocyclic boronates are key precursors for many cross-coupling reactions that are difficult to produce by conventional borylation strategies, due to the interference of electrophilic or coordinating heteroatom-centered residues. We, therefore, evaluated the performance of the new catalytic system with a wide range of heterocyclic precursors (Table 6). A wide range of substituted pyridineboronates (**75-84**), including those bearing unprotected amino group (**75**), fluoro (**78** and **79**), ester, cyano, trifluoromethyl and amido groups (**80-84**) were readily accessed. Borylated quinolines (**85-87**),

**Table 6. Scope of the Visible Light-Induced C–X Borylation Reaction of Haloheteroarenes.<sup>a</sup>**

<sup>a</sup> Reaction conditions: see footnote for Table 3 with 2 equiv. B<sub>2</sub>Pin<sub>2</sub>, X = Br unless otherwise specified. <sup>b</sup> 3 equiv. B<sub>2</sub>Pin<sub>2</sub>.

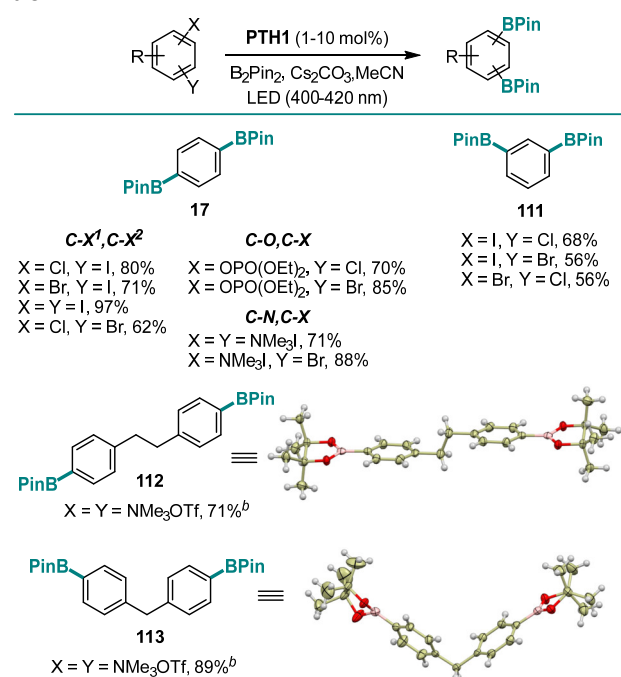
**Table 7. Scope of the Visible Light-Induced C–X Borylation Reaction of APIs and Natural Products.<sup>a</sup>**

<sup>a</sup> Reaction conditions: see footnote for Table 3 with 2 equiv. B<sub>2</sub>Pin<sub>2</sub>. <sup>b</sup> 3 equiv. B<sub>2</sub>Pin<sub>2</sub>.

indoles, and carbazoles (**88-91**) were also synthesized in good yields. Since heterocycles that contain multiple nitrogen atoms present a challenge for conventional borylation methods, we evaluated the reaction performance with borylated heterocycles **92-95** and observed smooth conversion. Oxygen- and sulfur-containing heterocycles were also tolerated (**96-100**).

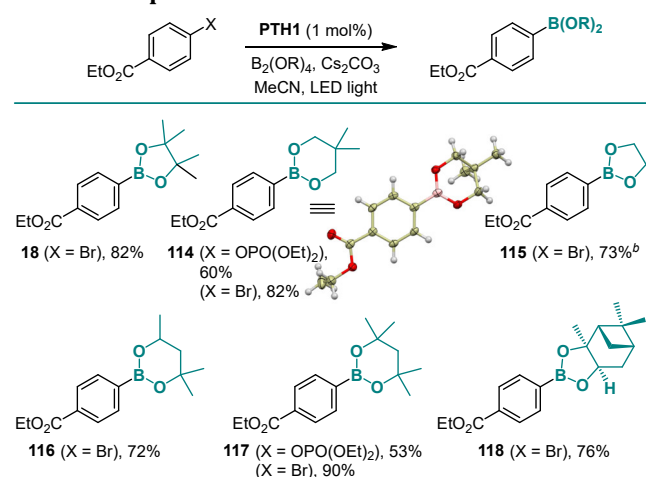
The new borylation preformed equally well in the more complex structural settings of natural products and APIs (Table 7).

Boronates derived from salicine (**101**), strychnine (**102**), as well as a variety of APIs and estrone (**35**, **103-110**) bearing basic heteroatoms, polar groups, and heterocyclic frameworks were readily synthesized, confirming versatility of the new method. The ability of the new catalytic system to effect the borylation of all five major classes of C–X bonds can be exploited for the simultaneous introduction of two boryl groups, en route to diborylarenes that have found applications as linchpins and phosphors in materials science.<sup>3</sup> Thus, various combinations of C–O, C–Cl, C–Br, C–I, and C–N bonds were

**Table 8. Scope of the Visible Light-Induced Dual Borylation.**<sup>a</sup>

<sup>a</sup> Reaction conditions: see footnote for Table 3. <sup>b</sup> The salt was prepared in situ by stirring the aniline precursor with MeOTf for 30 min at rt before adding B<sub>2</sub>Pin<sub>2</sub> and PTH1.

simultaneously borylated, providing a straightforward access to regioisomeric diborylarenes from a variety of halogenated phenols, anilines, as well as dihaloarenes, by-passing intermediates (Table 8, **17**, **111-113**). Additionally, we tested the performance of the catalytic system with a range of diboron esters (Table 9), since generation of various boryl esters using a single borylation protocol presents remains a challenge and is generally available only with UV-induced protocols. In all cases, a uniformly smooth performance was observed, and the corresponding products (**18**, **114-118**) were obtained in good yields. In contrast, B<sub>2</sub>(OH)<sub>4</sub> proved to be unsuitable, due to insolubility in acetonitrile. Boronic acids can still be prepared using the present method, as exemplified by product **48**, by a simple modification in the workup procedure (See SI).

**Table 9. Scope of the Boronate Esters.**<sup>a</sup>

<sup>a</sup> Reaction conditions: see footnote for Table 3 with 2 equiv. B<sub>2</sub>Pin<sub>2</sub>. <sup>b</sup> Isolated as boronic acid.

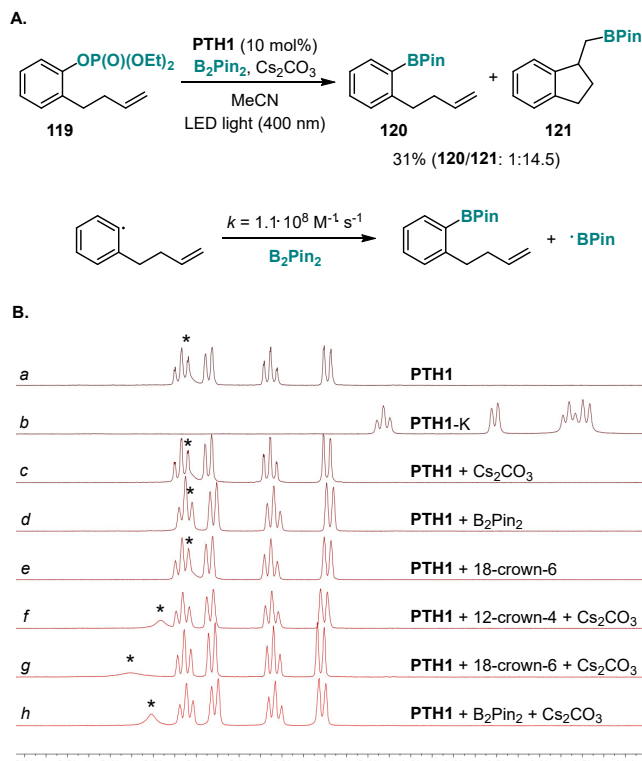


**Figure 2.** Mechanistic studies of the PTH1 photoredox catalyzed borylation reaction. **A.** Radical clock experiments with phosphate ester **119**. **B.** <sup>1</sup>H NMR spectra of PTH1 (*a*), potassium salt of PTH1 (PTH1-K, *b*), as well as PTH1 in the presence of Cs<sub>2</sub>CO<sub>3</sub>, B<sub>2</sub>Pin<sub>2</sub>, and crown ethers (*c-h*), in acetonitrile with a sealed coaxial capillary containing *d*<sub>12</sub>-cyclohexane.

Initial experimental observations of the pronounced *N*-substitution effects on the catalytic performance of phenothiazines PTH1-3 provided a strong indication of the crucial role of the N-H group for the photoredox catalysis by PTH1 (Table 1) that was also previously observed for other PCET-enabled catalytic systems.<sup>3f,g</sup> Furthermore, the acceleration observed with reagents that improve solubility and phase transfer of cesium carbonate also points to the equally important role of the base. We, therefore, conducted a series of experiments in order to clarify the mechanistic details of the photocatalysis. First, the aryl radical intermediacy was confirmed in radical clock experiments with phosphate **119** that produced boronates **120** and **121** (Figure 2.A). The bimolecular rate constant of the reaction of the aryl radical with B<sub>2</sub>pin<sub>2</sub> ( $k = 1.1 \cdot 10^8 \text{ M}^{-1} \cdot \text{s}^{-1}$ ) was comparable with the value reported by Studer ( $7.4 \cdot 10^7 \text{ M}^{-1} \cdot \text{s}^{-1}$ ) for the reaction of the catechol-derived diboron reagent B<sub>2</sub>Cat<sub>2</sub> with the aryl radical produced from the corresponding iodoarene.<sup>12</sup> We next examined the roles of cesium carbonate and the diboron reagent in the photoredox catalysis by PTH1 by means of <sup>1</sup>H NMR spectroscopy. First, formation of the phenothiazine anion from PTH1 in the presence of cesium carbonate was ruled out (Figure 2.B, PTH1-K, potassium salt of phenothiazine was used, cf. traces *a-c, h*), indicating that the reaction does not proceed by a stepwise mechanism with the phenothiazine anion acting as an electron donor in a photoinduced electron transfer. This conclusion was independently corroborated by UV/Vis studies of the PTH1/Cs<sub>2</sub>CO<sub>3</sub>/B<sub>2</sub>Pin<sub>2</sub> system (see SI). Further, no significant changes in the <sup>1</sup>H NMR spectrum of PTH1 were observed in the presence of B<sub>2</sub>Pin<sub>2</sub>, and only a minor shift of the N-H signal was observed in the PTH1-Cs<sub>2</sub>CO<sub>3</sub> system, as expected from the poor solubility of Cs<sub>2</sub>CO<sub>3</sub> in acetonitrile (cf. traces *a, c, d*). Significantly, addition of B<sub>2</sub>Pin<sub>2</sub> to the PTH1-Cs<sub>2</sub>CO<sub>3</sub>

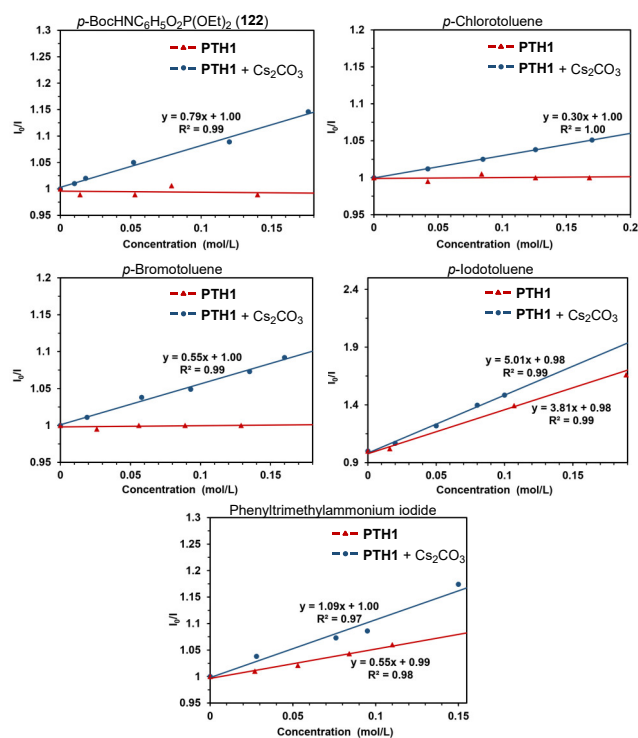


**Figure 3.** Fluorescence quenching experiments for **PTH1** in the presence and in the absence of cesium carbonate and 18-crown-6 with representative borylation substrates.

system led to a downfield shift of the N–H signal (cf. traces *c* and *h*). The same shift was observed for the **PTH1**– $\text{Cs}_2\text{CO}_3$  system in the presence of crown ethers (cf. traces *f*, *g*, and *h*). No interaction between **PTH1** and  $\text{B}_2\text{Pin}_2$  or crown ethers was observed in the absence of  $\text{Cs}_2\text{CO}_3$  (cf. traces *d*, *e* and *g*, *h*). These observations suggest that, in addition to the primary role as a borylation reagent,  $\text{B}_2\text{Pin}_2$  also serves as a phase transfer mediator for cesium carbonate, mimicking the behavior of crown ethers. In support of this conclusion, the  $\text{B}_2\text{Pin}_2$ – $\text{Cs}^+$  species was detected in the solution of **PTH1** in the presence of  $\text{Cs}_2\text{CO}_3$  and  $\text{B}_2\text{Pin}_2$  by HRMS (MW = 387.0920), while no signals corresponding to the  $sp^3$ -adduct of  $\text{B}_2\text{Pin}_2$  and  $\text{Cs}_2\text{CO}_3$  were detected by  $^{11}\text{B}$  NMR spectroscopy, indicating that  $\text{B}_2\text{Pin}_2$  primarily interacts with the base via the cesium ions. Taken together, these results suggest a hydrogen bonding interaction of **PTH1** and  $\text{Cs}_2\text{CO}_3$  that is assisted by  $\text{B}_2\text{Pin}_2$ . The role of the **PTH1**– $\text{Cs}_2\text{CO}_3$  interaction in the borylation was further probed by fluorescence quenching experiments with representative substrates (Ar–LG, LG =  $\text{O}_2\text{P}(\text{OEt})_2$ , Cl, Br, I,  $\text{NMe}_3\text{I}$ ) (Figure 3). For the purpose of the fluorescence quenching experiments, 18-crown-6 was used as a phase transfer mediator in place of  $\text{B}_2\text{Pin}_2$  to ensure that the quenching is not affected by the concomitant borylation, and given the similar behavior of the crown ester and  $\text{B}_2\text{Pin}_2$  (vide supra). As expected, no **PTH1** fluorescence quenching was observed with phosphate ester **122**<sup>20</sup> in the absence of  $\text{Cs}_2\text{CO}_3$  and the crown ether.<sup>21</sup> However, the fluorescence was quenched in the **PTH1**– $\text{Cs}_2\text{CO}_3$ –18-crown-6 system, pointing to the involvement of a **PTH1**–carbonate-enabled PCET process in the borylation. *p*-Chlorotoluene and *p*-bromotoluene exhibited similar quenching behavior, consistent with their low reduction potentials. Iodoarenes and arylammonium salts, on the other hand, have less negative reduction potentials, and direct photoinduced electron transfer from excited **PTH1** was anticipated to contribute to the borylation process. Indeed, **PTH1** fluorescence quenching was observed with *p*-iodotoluene. In line with the expected contribution of the

**PTH1**–carbonate-driven PCET process, stronger quenching was observed in the **PTH1**– $\text{Cs}_2\text{CO}_3$ –crown ether system. The same quenching behavior was observed for phenyltrimethylammonium iodide, as anticipated for the more readily reducible substrate. Taken together, the pronounced *N*-substitution effects combined with the results of the  $^1\text{H}$  NMR and fluorescence quenching studies suggest that the photoredox catalysis by **PTH1** is enabled by a proton-coupled electron transfer process arising from the **PTH1**–carbonate interaction exemplified by complex **123** (Figure 4), resulting in the borylation of substrates that have previously not been suitable for visible light-induced photoredox catalysis.

Thermodynamic and kinetic feasibility of the **PTH1**–carbonate photocatalytic borylation was further assessed computationally. (TD)DFT calculations show that the photoinduced proton-coupled electron transfer renders the one-electron reduction of aryl phosphate esters thermodynamically favorable from the singlet excited state of complex **123** (Figure 4, modelled with phosphate ester **124**). Furthermore, Marcus theory-based estimations suggest that the reduction may occur by a stepwise dissociative process,

proceeding with a low activation barrier (2.1 kcal/mol) via radical anion intermediate **124**<sup>•−</sup>. The subsequent homolytic substitution reaction of the generated aryl radical with  $\text{B}_2\text{Pin}_2$  also proceeds with a low barrier of 4.4 kcal/mol. Importantly, the ensuing barrierless and exergonic reaction of the intermediate boryl radical with the oxidized photocatalyst complex **125** (i.e., phenothiazinyl radical – hydrogen carbonate complex) provides a pathway for the regeneration of catalytically active complex **123**. The computational conclusions are consistent with the experimental observations and provide further support to the borylation mechanism.

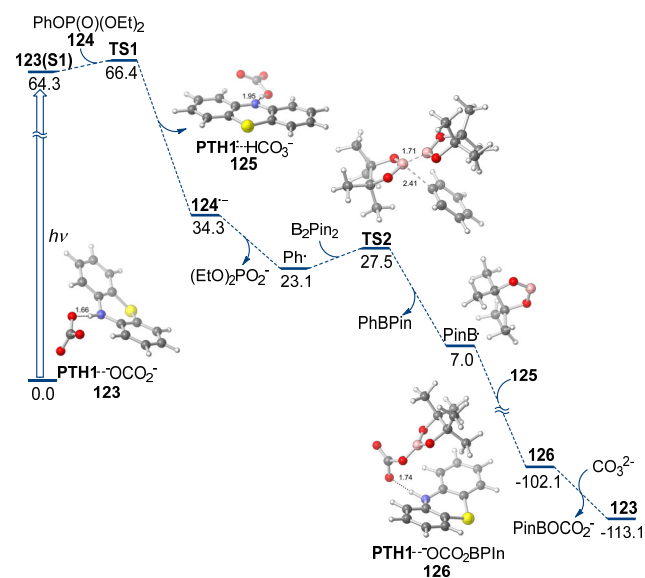


**Figure 4.** Computed Gibbs free energy profile of the **PTH1**-photoredox catalyzed borylation reaction of phosphate esters,  $\Delta\text{G}$ , kcal/mol.

## Conclusion

In conclusion, we have developed a metal-free, visible light-induced photocatalytic borylation platform that enables borylation of a range of carbon–heteroatom bonds, including, for the first time, C–O borylation of electron rich phenol derivatives, chloroarenes, and C–N borylation of aniline-derived quaternary ammonium salts. The scope and functional group

tolerance of the method were further demonstrated on a number of representative carbocyclic and heterocyclic substrates, as well as natural products and medicinally relevant compounds. The photocatalysis is enabled by the simple, abundant and low molecular weight heterocyclic commodity chemical phenothiazine **PTH1** that effects single electron reduction of substrates with strong bonds and low reduction potentials by a proton-coupled electron transfer mechanism.

## ASSOCIATED CONTENT

### Supporting Information

Experimental and spectral details for all new compounds and all reactions reported. This material is available free of charge via the Internet at <http://pubs.acs.org>.

## AUTHOR INFORMATION

### Corresponding Author

oleg.larionov@utsa.edu

### Notes

The authors declare no competing financial interest.

## ACKNOWLEDGMENT

Financial support by the Welch Foundation (AX-1788), NSF (CHE-1455061) and NIGMS (GM134371) is gratefully acknowledged. UTSA NMR and X-ray crystallography facilities were supported by NSF (CHE-1625963 and CHE-1920057). The authors acknowledge the Texas Advanced Computing Center (TACC) at UT Austin for providing computational resources.

## REFERENCES

(1) (a) Suzuki, A.; Brown, H. C. *Organic Syntheses Via Boranes*; Aldrich Chemical Company: Milwaukee, 2003; Vol. 3. (b) Hall, D. G. *Boronic Acids*, 2<sup>nd</sup> ed.; Wiley-VCH: Weinheim, 2011.

(2) (a) Corey, E. J. Catalytic Enantioselective Diels–Alder Reactions: Methods, Mechanistic Fundamentals, Pathways, and Applications. *Angew. Chem., Int. Ed.* **2002**, *41*, 1650. (b) Ishihara, K. Synthesis and Application of Organoboron Compounds. *Top. Organomet. Chem.* **2015**, *49*, 243.

(3) (a) Shoji, Y.; Iwabata, Y.; Wang, Q.; Nemoto, D.; Sakamoto, A.; Tanaka, N.; Seino, J.; Nakai, H.; Fukushima, T. Unveiling a New Aspect of Simple Arylboronic Esters: Long-Lived Room-Temperature Phosphorescence from Heavy-Atom-Free Molecules. *J. Am. Chem. Soc.* **2017**, *139*, 2728. (b) Huang, N.; Ding, X.; Kim, J.; Ihee, H.; Jiang, D. A Photoresponsive Smart Covalent Organic Framework. *Angew. Chem., Int. Ed.* **2015**, *54*, 8704.

(4) Ban, H. S.; Nakamura, H. Boron-Based Drug Design. *Chem. Rec.* **2015**, *15*, 616.

(5) Wu, J.; Kwon, B.; Liu, W.; Anslyn, E. V.; Wang, P.; Kim, J. S. Chromogenic/Fluorogenic Ensemble Chemosensing Systems. *Chem. Rev.* **2015**, *115*, 7893.

(6) (a) Cho, J.-Y.; Tse, M. K.; Holmes, D.; Maleczka, R. E.; Smith, M. R. Remarkably Selective Iridium Catalysts for the Elaboration of Aromatic C–H Bonds. *Science* **2002**, *295*, 305. (b) Mazzacano, T. J.; Mankad, N. P. Base Metal Catalysts for Photochemical C–H Borylation That Utilize Metal–Metal Cooperativity. *J. Am. Chem. Soc.* **2013**, *135*, 17258. (c) Molander, G. A.; Trice, S. L. J.; Dreher, S. D. Palladium-Catalyzed, Direct Boronic Acid Synthesis from Aryl Chlorides: A Simplified Route to Diverse Boronate Ester Derivatives. *J. Am. Chem. Soc.* **2010**, *132*, 17701. (d) Huang, K.; Yu, D.-G.; Zheng, S.-F.; Wu, Z.-H.; Shi Z.-J. Borylation of Aryl and Alkenyl Carbamates through Ni-Catalyzed C–O Activation. *Chem. Eur. J.* **2011**, *17*, 786. (e) Dudnik, A. S.; Fu, G. C. Nickel-Catalyzed Coupling Reactions of Alkyl Electrophiles, Including Unactivated Tertiary Halides, To Generate Carbon–Boron Bonds. *J. Am. Chem. Soc.* **2012**, *134*, 10693. (f) Nakamura, K.; Tobisu, M.; Chatani, N. Nickel-Catalyzed Formal Homocoupling of Methoxyarenes for the Synthesis of Symmetrical Biaryls via C–O Bond Cleavage. *Org. Lett.* **2015**, *17*, 6142. (g) Zarate, C.; Manzano, R.; Martin, R. Ipso-

Borylation of Aryl Ethers via Ni-Catalyzed C–OMe Cleavage. *J. Am. Chem. Soc.* **2015**, *137*, 6754. (h) Atack, T. C.; Cook, S. P. Manganese-Catalyzed Borylation of Unactivated Alkyl Chlorides. *J. Am. Chem. Soc.* **2016**, *138*, 6139. (i) Yoshida, T.; Iliès, L.; Nakamura, E. Iron-catalyzed Borylation of Aryl Chlorides in the Presence of Potassium *t*-Butoxide. *ACS Catal.* **2017**, *7*, 3199. (j) Li, C.; Wang, J.; Barton, L. M.; Yu, S.; Tian, M.; Peters, D. S.; Kumar, M.; Yu, A. W.; Johnson, K. A.; Chatterjee, A. K.; Yan, M.; Baran, P. S. Decarboxylative Borylation. *Science* **2017**, *356*, eaam7355. (k) Arevalo, R.; Chirik, P. J. Enabling Two-Electron Pathways with Iron and Cobalt: From Ligand Design to Catalytic Applications. *J. Am. Chem. Soc.* **2019**, *141*, 9106. (l) Malapit, C. A.; Bour, J. R.; Laursen, S. R.; Sanford, M. S. Mechanism and Scope of Nickel-Catalyzed Decarboxylative Borylation of Carboxylic Acid Fluorides. *J. Am. Chem. Soc.* **2019**, *141*, 17322.

(7) (a) Nagashima, Y.; Takita, R.; Yoshida, K.; Hirano, K.; Uchiyama, M. Design, Generation, and Synthetic Application of Borylzincate: Borylation of Aryl Halides and Borylzincation of Benzyne/Terminal Alkyne. *J. Am. Chem. Soc.* **2013**, *135*, 18730. (b) Bose, S. K.; Fucke, K.; Liu, L.; Steel, P. G.; Marder, T. B. Zinc-Catalyzed Borylation of Primary, Secondary and Tertiary Alkyl Halides with Alkoxy Diboron Reagents at Room Temperature. *Angew. Chem., Int. Ed.* **2014**, *53*, 1799. (c) Warner, A. J.; Lawson, J. R.; Fasano, V.; Ingleson, M. J. Formation of C(sp<sup>2</sup>)-Boronate Esters by Borylative Cyclization of Alkynes Using BCl<sub>3</sub>. *Angew. Chem., Int. Ed.* **2015**, *54*, 11245. (d) Légare, M. A.; Courtemanche, M. A.; Rochette, É.; Fontaine, F. G. Metal-Free Catalytic C–H Bond Activation and Borylation of Heteroarenes. *Science* **2015**, *349*, 513. (e) Mo, F.; Qiu, D.; Zhang, Y.; Wang, J. Renaissance of Sandmeyer-Type Reactions: Conversion of Aromatic C–N Bonds into C–X Bonds (X = B, Sn, P, or CF<sub>3</sub>). *Acc. Chem. Res.* **2018**, *51*, 496. (f) Zhang, L.; Jiao, L. Pyridine-Catalyzed Radical Borylation of Aryl Halides. *J. Am. Chem. Soc.* **2017**, *139*, 607. (g) Zhang, L.; Jiao, L. Super Electron Donors Derived from Diboron. *Chem. Sci.* **2018**, *9*, 2711. (h) Su, Y.; Cao, D.; Do, H.; Li, Y.; Kinjo, R. Metal-Free Selective Borylation of Arenes by a Diazadiborinane via C–H/C–F Bond Activation and Dearomatization. *J. Am. Chem. Soc.* **2019**, *141*, 13729. (i) Lv, J.; Chen, X.; Xue, X.-S.; Zhao, B.; Liang, Y.; Wang, M.; Jin, L.; Yuan, Y.; Han, Y.; Zhao, Y.; Lu, Y.; Zhao, J.; Sun, W.-Y.; Houk, K. N.; Shi, Z. Metal-Free Directed sp<sup>2</sup>-C–H Borylation. *Nature* **2019**, *575*, 336.

(8) (a) Mfuh, A. M.; Doyle, J. D.; Chhetri, B.; Arman, H. D.; Larionov, O. V. Scalable, Metal- and Additive-Free, Photoinduced Borylation of Haloarenes and Quaternary Arylammonium Salts. *J. Am. Chem. Soc.* **2016**, *138*, 2985. (b) Chen, K.; Zhang, S.; He, P.; Li, P. Efficient Metal-Free Photochemical Borylation of Aryl Halides under Batch and Continuous-Flow Conditions. *Chem. Sci.* **2016**, *7*, 3676.

(9) Liu, W.; Yang, X.; Gao, Y.; Li, C.-J. Simple and Efficient Generation of Aryl Radicals from Aryl Triflates: Synthesis of Aryl Boronates and Aryl Iodides at Room Temperature. *J. Am. Chem. Soc.* **2017**, *139*, 8621.

(10) Zhang, L.; Jiao, L. Visible-Light-Induced Organocatalytic Borylation of Aryl Chlorides. *J. Am. Chem. Soc.* **2019**, *141*, 9124.

(11) Qiao, Y.; Yang, Q.; Schelter, E. Photoinduced Miyaura Borylation by a Rare Earth Photoreductant: the Hexachloroacetate(III) Anion. *Angew. Chem., Int. Ed.* **2018**, *57*, 10999.

(12) Cheng, Y.; Mück-Lichtenfeld, C.; Studer, A. Metal-Free Radical Borylation of Alkyl and Aryl Iodides. *Angew. Chem. Int. Ed.* **2018**, *57*, 16832.

(13) (a) Cheung, M. S.; Lin, Z.; Li, P. Metal-Free Borylation of Electron-Rich Aryl (Pseudo)halides under Continuous-Flow Photolytic Conditions. *Org. Chem. Front.* **2016**, *3*, 875. (b) Candish, L.; Teders, M.; Glorius, F. Transition-Metal-Free, Visible-Light-Enabled Decarboxylative Borylation of Aryl *N*-Hydroxyphthalimide Esters. *J. Am. Chem. Soc.* **2017**, *139*, 7440. (c) Fawcett, A.; Pradeilles, J.; Wang, Y.; Mutsuga, T.; Myers, E. L.; Aggarwal, V. K. Photoinduced Decarboxylative Borylation of Carboxylic Acids. *Science* **2017**, *357*, 283. (d) Jin, S.; Nguyen, V. T.; Dang, H. T.; Nguyen, D. P.; Arman, H. D.; Larionov, O. V. Photoinduced Carboborane Ring Contraction Enables Regio- and Stereoselective Synthesis of Multiply Substituted Five-Membered Carbocycles and Heterocycles. *J. Am. Chem. Soc.* **2017**, *139*, 11365. (e) Hu, D.; Wang, L.; Li, P. Decarboxylative Borylation of Aliphatic Esters under Visible-Light Photoredox Conditions. *Org. Lett.* **2017**, *19*, 2770. (f) Wu, J.; He, L.; Noble, A.; Aggarwal, V. K. Photoinduced Deaminative Borylation of Alkylamines. *J. Am. Chem. Soc.* **2018**, *140*, 10700. (g) Cheng, Y.; Mück-Lichtenfeld, C.; Studer, A. Transition Metal-Free 1,2-Carboboration of Unactivated Alkenes. *J. Am. Chem. Soc.* **2018**, *140*, 6221. (h) Friese, F. W.; Studer, A. Deoxygenative Borylation of Secondary and Tertiary

Alcohols. *Angew. Chem. Int. Ed.* **2019**, *58*, 9561. (i) Wu, J.; Baer, R.; Guo, L.; Noble, A.; Aggarwal, V. K. Photoinduced Deoxygenative Borylations of Aliphatic Alcohols. *Angew. Chem. Int. Ed.* **2019**, *58*, 18830. (j) Mazzarella, D.; Magagnano, G.; Schweitzer-Chaput, B.; Melchiorre, P. Photochemical Organocatalytic Borylation of Alkyl Chlorides, Bromides, and Sulfonates. *ACS Catal.* **2019**, *9*, 5876. For reviews, see: (k) Nguyen, V. D.; Nguyen, V. T.; Jin, S.; Dang, H. T.; Larionov, O. V. Organoboron Chemistry Comes to Light: Recent Advances in Photoinduced Synthetic Approaches to Organoboron Compounds. *Tetrahedron* **2019**, *75*, 584. (l) Friese, F. W.; Studer, A. New Avenues for C–B Bond Formation via Radical Intermediates. *Chem. Sci.* **2019**, *10*, 8503. (m) Liu, W.; Li, J.; Huang, C.-Y.; Li, C.-J. Aromatic Chemistry in the Excited State: Facilitating Metal-Free Substitutions and Cross-Couplings. *Angew. Chem. Int. Ed.* **2019**, DOI: 10.1002/anie.201909138.

(14) Luo, Y.-R. *Comprehensive Handbook of Chemical Bond Energies*; CRC Press: Boca Raton, FL, 2007.

(15) Photochemistry of Phosphate and Sulfonate Esters. Ravelli, D.; Fagnoni, M. In *CRC Handbook of Organic Photochemistry and Photobiology*, 3<sup>rd</sup> Ed.; Griesbeck, A. G.; Oelgemöller, M.; Ghetti, F.; Eds.; CRC Press: Boca Raton, 2012.

(16) All reduction potentials are reported vs SCE in acetonitrile.

(17) (a) Choi, G. J.; Zhu, Q.; Miller, D. C.; Gu, C. J.; Knowles, R. R. Catalytic Alkylation of Remote C–H Bonds Enabled by Proton-Coupled Electron Transfer. *Nature* **2016**, *539*, 268. (b) Yayla, H. G.; Wang, H.; Tarantino, K. T.; Orbe, H. S.; Knowles, R. R. Catalytic Ring-Opening of Cyclic Alcohols Enabled by PCET Activation of Strong O–H Bonds. *J. Am. Chem. Soc.* **2016**, *138*, 10794. (c) Chen, M.; Zhao, X.; Yang, C.; Xia, W. Visible-light-triggered directly reductive arylation of carbonyl/iminyl derivatives through photocatalytic PCET. *Org. Lett.* **2017**, *19*, 3807. (d) Nguyen, V. D.; Nguyen, V. T.; Haug, G. C.; Dang, H. T.; Jin, S.; Li, Z.; Flores-Hansen, C.; Benavides, B.; Arman, H. D.; Larionov, O. V. *ACS Catal.* **2019**, *9*, 9485. (e) Morton, C. M.; Zhu, Q.; Ripberger, H.; Troian-Gautier, L.; Toa, Z. S. D.; Knowles, R. R.; Alexanian, E. J. C–H Alkylation via Multisite Proton-Coupled Electron Transfer of an Aliphatic C–H Bond. *J. Am. Chem. Soc.* **2019**, *141*, 13253. For reviews, see: (f) Gentry, E. C.; Knowles, R. R. Synthetic Applications of Proton-Coupled Electron Transfer. *Acc. Chem. Res.* **2016**, *49*, 1546. (g) Hoffmann, N. Proton-Coupled Electron Transfer in Photoredox Catalytic Reactions. *Eur. J. Org. Chem.* **2017**, *15*, 1982.

(18) (a) Treat, N. J.; Sprafke, H.; Kramer, J. W.; Clark, P. G.; Barton, B. E.; Read de Alaniz, J.; Fors, B. P.; Hawker, C. J. Metal-Free Atom Transfer Radical Polymerization. *J. Am. Chem. Soc.* **2014**, *136*, 16096. (b) Pan, X.; Lamson, M.; Yan, J.; Matyjaszewski, K. Photoinduced Metal-Free Atom Transfer Radical Polymerization of Acrylonitrile. *ACS Macro Lett.* **2015**, *4*, 192. (c) Discekici, E. H.; Treat, N. J.; Poelma, S. O.; Mattson, K. M.; Hudson, Z. M.; Luo, Y.; Hawker, C. J.; Read de Alaniz, J. A Highly Reducing Metal-Free Photoredox Catalyst: Design and Application in Radical Dehalogenation. *Chem. Comm.* **2015**, *51*, 11705. (d) Martínez-Gualda, A. M.; Cano, R.; Marzo, L.; Pérez-Ruiz, R.; Luis-Barrera, J.; Mas-Ballesté, R.; Fraile, A.; de la Peña O'Shea, V. A.; Alemán, J. Chromoselective Access to *Z*- or *E*- Allylated Amines and Heterocycles by a Photocatalytic Allylation Reaction. *Nat. Commun.* **2019**, *10*, 2634. (e) Boyington, A. J.; Seath, C. P.; Zearfoss, A. M.; Xu, Z.; Jui, N. T. Catalytic Strategy for Regioselective Arylethylamine Synthesis. *J. Am. Chem. Soc.* **2019**, *141*, 4147.

(19) Molander, G. A.; Ellis, N. Organotrifluoroborates: Protected Boronic Acids that Expand the Versatility of the Suzuki Coupling Reaction. *Acc. Chem. Res.* **2007**, *40*, 275.

(20) Phosphate **122** was used because of the interference of phosphate **1**-induced fluorescence at higher concentrations.

(21) No quenching was observed when either Cs<sub>2</sub>CO<sub>3</sub> or 18-crown-6 was absent.

### TOC graphic

